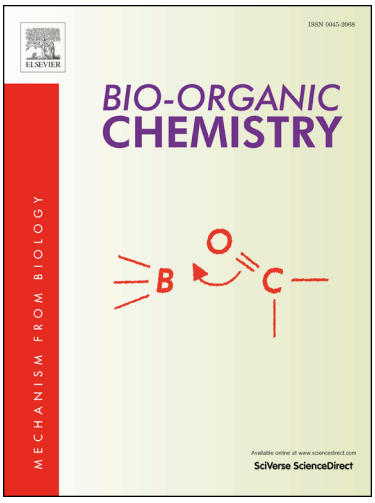

[12]aneN$_3$-based lipid with naphthalimide moiety for enhanced gene transfection efficiency

Yong-Guang Gao, Uzair Alam, Ai-Xiang Ding, QuanTang, Zheng-Li Tan, You-Di Shi, Zhong-Lin Lu, Ai-Rong Qian

PII: S0045-2068(18)30256-6
DOI: https://doi.org/10.1016/j.bioorg.2018.04.018
Reference: YBIOO 2341

To appear in: *Bioorganic Chemistry*

Received Date: 6 March 2018
Revised Date: 16 April 2018
Accepted Date: 24 April 2018

Please cite this article as: Y-G. Gao, U. Alam, A-X. Ding, QuanTang, Z-L. Tan, Y-D. Shi, Z-L. Lu, A-R. Qian, [12]aneN$_3$-based lipid with naphthalimide moiety for enhanced gene transfection efficiency, *Bioorganic Chemistry* (2018), doi: https://doi.org/10.1016/j.bioorg.2018.04.018

***[12]aneN$_3$-based lipid with naphthalimide moiety for enhanced gene transfection efficiency

Yong-Guang Gao[a,b], Uzair Alam[b], Ai-Xiang Ding[c], QuanTang[b], Zheng-Li Tan[b], You-Di Shi[b], Zhong-Lin Lu[b,*,luzl@bnu.edu.cn], Ai-Rong Qian[a,*,qianair@nwpu.edu.cn]

[a]Laboratory for Bone Metabolism, Key Laboratory for Space Bioscience and Biotechnology, School of Life Sciences, Northwestern Polytechnical University, Xi'an, Shaanxi 710072, China.
[b]KeyLaboratory of Theoretical and Computational Photochemistry, Ministry of Education, College of Chemistry, Beijing Normal University, Xinjiekouwai Street 19, Beijing 100875, China.
[c]Xinyang Normal University, Xinyang, Henan, China, 464000

[*]Corresponding authors.

Graphical abstract

Highlights

- The effect of the rigid naphthalimide moiety and flexible aliphatic chain on gene transfection efficiency was investigated.
- The lipid with rigid naphthalimide **1a** exhibited strong DNA binding ability and could effectively condense DNA into homogeneous square shaped nanoparticles.
- *Lipid **1a** showed excellent gene transfection efficiency and serum tolerance.*

Abstract
Three cationic lipids derived from ***[12]aneN$_3$ modified with naphthalimide (**1a**), oleic acid (**1b**) and octadecylamine (**1c**) were designed and synthesized. *In vitro* transfection showed that all these liposomes can deliver plasmid DNA into the tested cell lines. Among these liposomes, **1a** gave the best transfection efficiency (TE) in A549 cells, which was higher than that of lipofectamine 2000. More importantly, the TE of **1a** was dramatically increased in the presence of 10% serum. These results suggested that **1a** might be a promising non-viral gene vector, and also give further insight for developing novel high performance gene delivery agents.

Keywords:
non-viral vectors, cationic lipids, transfection efficiency, ***[12]aneN3, naphthalimide

1. Introduction

Gene therapy is a promising strategy in the treatment of genetic diseases and has attracted significant interest in clinical trials over the past two decades[1-8]. However, it is greatly limited due to the lack of nontoxic and high efficient gene delivery vectors[9]. Previously, viral vectors such as adenoviruses, lentiviruses and retroviruses have been successfully applied in several clinical applications because of their effective gene delivery ability[10-14], but their inherent drawbacks such as carcinogenicity, immunogenicity and difficulty of industrial production restrained them from therapeutic applications in humanp[15]. In contrast, non-viral vectors such as cationic lipids, cationic polymers and nanoparticles have received increased attention due to their low immunogenicity, good biocompatibility and easy production as well[16-26]. Among these non-viral vectors, cationic polymers show high transfection efficiency. However the usage of cationic polymers in applications in gene delivery is generally limited because of their high toxicity and non-degradable nature. In comparison, cationic lipids hold great potential for clinical gene therapy.

Cationic lipids as a type of important and potential non-viral gene vectors possess more advantages such as biodegradability, low cytotoxicity, structure variety and easy production etc[27, 28]. Though these advantages of

cationic lipids appear attractive, still low transfection efficiency and serum stability cannot satisfy the requirements of gene therapy. To improve the performance of cationic lipids, different kinds of aliphatic chains were used as hydrophobic domain of cationic lipids. The structure−activity correlations of cationic lipids were also studied. But these studies usually focus on changing the length and number of aliphatic chains[29]. The effects of big rigid aromatic units and flexible aliphatic chains on transfection efficiency have been seldom studied.

Recently, we developed a series of ***[12]aneN_3 cationic lipids modified with different rigid units such as naphthalimide, tetraphenylethene and coumarin[30-33]. It was found that the transfection efficiency was related to the number of rigid moieties and macrocyclic polyamine ***[12]aneN_3 units[31, 33], as well as to the distance between naphthalimide moiety and ***[12]aneN_3 units[32]. Moreover, rigid naphthalimide unit, possessing strong green fluorescence and exceptional photo-stability, can be applied for monitoring the process of cellular uptake, DNA translocation and release[30]. However, these works have just focused on rigid units, while the flexible aliphatic chains had been ignored. To compare the difference between long flexible aliphatic chains and big rigid aromatic unit, we designed and synthesized three cationic lipids containing rigid naphthalimide unit (**1a**), unsaturated aliphatic chain (**1b**) and saturated aliphatic chain (**1c**). Due to good fluorescence properties of **1a**, the distribution of **1a**/DNA complexes and cellular uptake mechanism studies can be easily carried out through fluorescence microscopy. On the other hand, non-fluorescent compounds **1b** and **1c** can be applied in green fluorescent protein (eGFP) experiments. Among these lipids, **1a** gave the best transfection efficiency (TE) in A549 cells and exhibited good serum-tolerance ability, indicating that **1a** may serve as a promising non-viral gene delivery vector.

2. Results and discussion

*2.1 Synthesis of target cationic lipids **1a-1c***

Target lipids **1a**, **1b** and **1c** were synthesized as shown in Scheme 1. The key intermediate Boc-protected ***[12]aneN_3 **5** was obtained through two steps. 1,3-bis(bromomethyl)-5-nitrobenzene **2[**34**]** was reacted with pre***-[12]aneN_3 **3** in anhydrous acetonitrile, followed by acidification with 3M HCl solution and protection with Boc_2O to give compound **4**. Subsequently, the reaction of **4** with hydrazine hydrate in presence of 10% Pd/C yielded the key intermediate **5**. Compounds **5** and **6** were easily linked by triphosgene under basic conditions and further de-protection of Boc under acidic conditions resulted target compound **1a**. Compound **1b** was obtained by reaction of oleic acid **7** with compound **5** in the presence of (1-ethyl-3-(3-dimethylaminopropyl) carbodiimide hydrochloride) (EDC·HCl) and *N*-hydroxybenzotriazole (HOBt). 3,5-bis(azidomethyl)benzoic acid **8[**30**]** was reacted with octadecylamine in dichloromethane to produce the key intermediate *N*-(3,5-bis(azidomethyl)phenyl)stearamide. Subsequently, the click reaction of the key intermediate with propargyl ***[12]aneN_3 **9[**35**]** and de-protection of Boc under acidic conditions resulted in target cationic lipid **1c**. All new compounds were fully characterized by ^{1}H NMR, ^{13}C NMR, IR and MS**.**

2.2 Gel retardation assay

Cationic liposomes were formed from the combination of title lipids with 1,2-dioleoyl-*sn*-glycero-3-phosphoethanolamine (DOPE) in the molar ratio of 1:2. To investigate the interaction between liposomes and DNA, agarose gel electrophoresis assays were carried out in HEPES buffer (50 mM, pH 7.4) at 37 °C (Fig. 1). The results indicated that liposomes **1a (**containing rigid naphthalimide unit) and **1c** had stronger DNA retardation activity than **1b**, with complete retardation observed at concentrations of 20 μM, 20 μM and 50 μM, respectively. The weaker retardation activity of **1b** can be attributed to the presence of electron-rich unsaturated alkyl chain, which could shield the positive charge of the liposome[36].

2.3 Dynamic light scattering

It is well known that gene delivery ability is greatly affected by particle size of the liposome/DNA complexes. Dynamic light scattering (DLS) was used to characterize the size distribution of lipoplexes. As shown in Fig. 2, the liposomes of **1a-1c** could efficiently condense DNA into nanoparticles with diameters in the range of 50–160 nm at the concentrations ranging from 5 to 40 μM. The particle size seemed to be suitable for cell endocytosis and further gene transfection experiments[37, 38]. It was also observed that the size of condensed DNA particles increased significantly with increasing concentrations of compound **1a**. As we all know, the formation of nanoparticles can be attributed to the combination effects caused by electrostatic forces, intercalation between the adjacent DNA base pairs, as well as to the π-stacking interactions between rigid units and nucleotides. In **1a**/DNA complexes, π-π stacking interaction between compound **1a** and DNA might play a dominant role as compared to electrostatic forces,

which was solely the reason for the increased size of **1a**/DNA complexes with increasing concentrations of compound **1a**.

2.4 Scanning electron microscopy

The morphology of DNA condensates also played an important role in gene delivery. Scanning electron microscope (SEM) was applied to get the information about morphology of liposome **1a**/DNA complexes at different concentrations of 5-40 μM. As shown in Fig. 3, liposome **1a** can effectively condense DNA into homogeneous square shaped nanoparticles, and the size of nanoparticles was gradually increased with increasing concentration of compound **1a,** which was consistent with the results of DLS assay. According to the literature report, the colipid DOPE could increase the stability of the lipoplexes, and help lipid to form various structural phases, such as the micellar, lamellar, cubic, and inverted hexagonal phase, and arrange back-to-back in bilayers[29]. It is possible that π-π stacking interactions between rigid naphthalimide and nucleotides may have a strong tendency to form a homogeneous square nanostructure. Furthermore, nanoparticle sizes measured by SEM (30-120 nm) were smaller than those obtained by DLS (50-160 nm), which could be attributed to different methods for the preparation of liposome/DNA complexes[39, 40]. The hydrated complex was examined by DLS, while dehydrated was measured by SEM.

2.5 Cytotoxicity assay

The cytotoxicity of gene delivery agents is a key index for their potential clinical applications. Thus the cytotoxicity of liposomes **1a**, **1b** and **1c** towards A549, HeLa, U2Os and SKOV-3 cells was investigated by using MTT assays, and lipofectamine 2000 was used as control. The results (Fig. 4) revealed that percentage of viable cells decreased with increasing concentrations of all the three liposomes. However, even at higher concentration, all three liposomes exhibited acceptable biocompatibility with 60 % viable cells were still present at 40 μM in all cell lines, which was suitable for further gene transfection.

2.6 In vitro transfection by liposomes

To further investigate the transfection ability of the liposomes as non-viral gene vectors, firstly liposomes **1a**, **1b** and **1c** mediated luciferase assay was conducted at different concentrations in A549 cells. As shown in Fig. 5A, these three liposomes exhibited the best transfection efficiency at the concentration of 30 μM, but at higher concentrations of liposomes, transfection efficiency was decreased because of the increased cytotoxicity. Among the liposomes, **1a** modified with rigid naphthalimide exhibited the best transfection efficiency, which was slightly higher than that of lipofectamine 2000. Compared to **1c**, the liposome of **1b** with an unsaturated aliphatic chain exhibited higher transfection efficiency, showing that the suitable DNA release ability was resulted from unsaturated aliphatic chain which might promote gene transfection[29]. Furthermore, the gene transfections mediated by **1a**, **1b** and **1c** were also performed at the concentration of 30 μM in other cell lines, and the results are shown in Fig. 5B. The liposome of **1a** showed the highest transfection efficiency in A549 cells. In contrast, other liposomes (**1b** and **1c**) had lower transfection efficiencies as compared with lipofectamine 2000. Subsequently, the gene transfection of liposome **1a** in the presence of fetal bovine serum (FBS) was investigated (Fig. 5C). As it can be seen from the figure, in the presence of 10% serum, the transfection efficiency of **1a** was dramatically increased 3 times as compared with the TE of **1a** in absence of serum. The good serum tolerance of liposome **1a** is probably attributed to the rigid aromatic moiety, which may enhance the resistance to serum-induced aggregation or premature DNA release[41-43]. Moreover, increased concentration of FBS resulted in decreased transfection efficiency of liposome **1a**. In order to study the stability of liposome **1a**/DNA complexes in the presence of fetal bovine serum, gel electrophoresis was carried out. **1a**/DNA complexes were incubated with 10%, 30% and 50% serum for 0.5 h. As shown in Fig. S1, DNA was found to be gradually released with the increase of serum. It was also observed that **1a**/DNA complexes could remain stable after 24 h incubation (Fig. S2), indicating good serum tolerance of liposome **1a**. To directly visualize the infected cells expressing pEGFP-Nl reporter gene, the liposomes **1b** and **1c** (30 μM) mediated enhanced green fluorescent protein (eGFP) expression in A549 cells was observed. As shown in Fig. 6, **1b**-promoted transfection produced higher fluorescence emission than **1c** at 30 μM concentration, which was consistent with the luciferase gene expression experiments.

2.7 Cellular uptake assays

To further examine the gene delivery ability of liposome **1a** in serum, cellular uptake assays were carried out in A549 cells using Cy5-labeled dsDNA. The gene delivery agent **1a** exhibited strong fluorescent emission at 551 nm (Fig.S3), while Cy5-labeled *ds*DNA emitted red fluorescence under fluorescence microscope. A common blue fluorescent dye DAPI was used to stain the nuclei of cells. As shown in Fig. 7, Cy5-DNA could be delivered into A549 cells with or without serum, but concentrations of the serum had an obvious influence on cellular uptake. It is obvious that the strongest fluorescence of **1a** and Cy5-DNA was observed simultaneously in the presence of 10% serum and the fluorescence intensity was gradually decreased with increasing concentrations of serum. When 50% serum was used as medium, almost no red fluorescent spot was observed, and the green fluorescence was also much weaker than that observed in 10% serum. These above results were in accordance with gene transfection experiments, indicating that serum had a significant effect both in the cellular uptake and gene transfection.

2.8 Mechanism Studies

It is a well-known fact that gene transfection is affected by several factors, such as temperature, cellular uptake level and internalization pathway. Endocytosis as a general entry mechanism is an energy-dependent uptake which can be blocked at low temperature (4 °C instead of 37 °C)[44, 45]. Cellular incubations with **1a**/DNA complexes were carried out at 4 °C and 37 °C. As shown in Fig. 8B, the fluorescence of **1a** was almost completely quenched after incubation for 2h at 4 °C, suggesting that **1a**-mediated endocytosis as the internalization mechanism is an energy-dependent uptake. Furthermore, the cellular uptake pathways of clathrin, macropinocytosis, caveolae, and microtubule mediated endocytosis could effectively be inhibited by chlorpromazine, cytochalasin D, genistein and nocodazole, respectively[46]. Therefore, we studied the influence of different chemical inhibitors on cellular uptake pathways. Results revealed that chlorpromazine, cytochalasin D and genistein had no obvious inhibiting effect on cellular uptake (Figs. 8C, 8D and 8F), suggesting that **1a**-mediated transfection was not dependent on clathrin, macropinocytosis and caveolae mediated endocytosis. The cellular uptake level was significantly inhibited by nocodazole (Fig. 8E), indicating that the cellular uptake proceeded via a microtubule-mediated endocytosis.

3. Conclusion

In conclusion, three cationic lipids **1a-1c** bearing different kinds of hydrophobic moieties were designed and synthesized through multistep reactions. These lipids were mixed with DOPE in the ratio of 1:2 to form corresponding liposomes, which could efficiently condense DNA into square shaped nanoparticles with the size in the range of 50–160 nm. *In vitro* gene transfection experiments indicated that all these liposomes could effectively deliver gene into different cell lines. Amongst them, **1a** with big rigid naphthalimide moiety exhibited the highest transfection efficiency, which was higher than that of lipofectamine 2000 in A549 cells. More importantly, **1a** showed excellent serum tolerance, as its transfection efficiency was increased 3 folds in the presence of 10% fetal bovine serum, indicating its good potential as promising gene vector *in vivo* application.

4. Experimental section

4.1 Physical Measurements

^{1}H and ^{13}C NMR spectra were obtained on a Bruker Avance III 400 MHz spectrometer at 25 ^{o}C. Chemical shifts were referenced on residual solvents peaks. The infrared spectra were taken on a Nicolet 380 spectrometer in the range of 4000-400 cm^{-1}. Mass spectra were acquired on a Waters Quattro Mocro spectrometer and high resolution mass spectra were acquired on a Waters LCT Premier XE spectrometer. Electrophoresis apparatus was a BG-subMIDI sub marine system (Baygene Biotech Company Limited, Beijing, China). Bands were visualized by UV light and recorded on a UVP EC3 visible imaging system. Hydrodynamic diameters were determined using a Brook Haven Zeta Plus Partical Size and Zeta Potential Analyzer. The morphologies of the lipoplexes were observed by SEM (aHitachi, X 650).

4.2 Chemicals

Anhydrous dichloromethane (DCM) was purified and dried under nitrogen by using standard methods and was distilled immediately before use. All other reagents were of analytical grade and were used as received. Pre***-[12]aneN_3 (compound **3**), 3,5-bis(azidomethyl) benzoic acid (compound **8**) and di-tert-butyl 9-(prop-2-ynyl)-1,5,9-triazacyclododecane-1,5-dicarboxylate (compound **9**) were prepared according to the literature[34, 35, 47]. Electrophoresis grade agarose, 6 × loading buffer, Goldview II, 3-(4,5-dimethylthiazol-2-yl)-2,5-diphenyltetrazolium bormide (MTT), plasmid DNA (pUC 18) were purchased from Beijing Solarbio Science& Technology Co. Ltd. (Beijing, China), 1,2-dioleoyl-*sn*-glycero-3-phosphoethanolamine (DOPE) was bought from Santa Cruz Biotechnology, Inc. (Texas, USA). Lipofectamine 2000^{TM} and plasmid PGL-3 vector were purchased from Clontech Laboratories, Inc. (Beijing, China). Ultrapure milli-Q water (18.25 MΩ) was used in all DNA condensation assays.

4.3 Synthesis

*4.3.1 Preparation of compound **4***

To a solution of 1,3-bis(bromomethyl)-5-nitrobenzene **2** (3.30 g, 10.68 mmol) in anhydrous acetonitrile (50 mL) was added pre***-[12]aneN_3 **3** (4.00 g, 22.07 mmol). The mixture was heated at 80 °C for 12 h. After cooling to room temperature, blue precipitates were filtered and washed with diethyl ether (30 mL) to obtain white solid. The above crude intermediate was added to 3 M hydrogen chloride solution (60 mL) and then refluxed for 12 h. The solvent was removed by reduced pressure to give white solid, which was added to a solution of Et_3N (5.11 g, 50.50 mmol) in dichloromethane (30 mL). Boc_2O (4.00 g, 18.33 mmol) was added in above mixture in small portions druing half an hour and stirred for 24 h. The mixture was concentrated to dryness and extracted with dichloromethane (3 × 30 mL). The combined organic layers were washed with water (3 × 10 mL) and dried over anhydrous Na_2SO_4. After filtration and concentration to dryness, the residue was purified by chromatography on silica gel (ethyl acetate/petroleum ether = 1/1) to give compound **4** (3.60 g, 38%) as yellow solid. ^{1}H NMR (400 MHz, $CDCl_3$) δ 8.05 (s, 2H), 7.49 (s, 1H), 3.61 (s, 4H), 3.40-3.31 (m, 16H), 2.51-2.35 (m, 8H), 1.97-1.86 (m, 4H), 1.85-1.74 (m, 8H), 1.44 (s, 36H). ^{13}C NMR (101 MHz, $CDCl_3$) δ 155.27, 147.53, 140.78, 133.96, 121.24, 78.51, 57.36, 48.96, 43.96, 42.69, 27.55, 26.69, 25.68. IR (KBr, cm^{-1}): 3433, 2971, 2938, 2797, 1691, 1532, 1472, 1411, 1349, 1250, 1202, 1159, 1068, 854, 564. ESI-MS Cacld. for $C_{46}H_{80}N_7O_{10}(M+H)^+$: 890.6, found: 890.9.

*4.3.2 Preparation of compound **5***

To a solution of compound **4** (2.40 g, 2.70 mmol) in methanol (25 mL) was added Pd/C (0.24 g , 10% w/w), and hydrazine hydrate (20 mL , 330.2 mmol). The mixture was heated to 75 °C for 10 h under N_2. After cooling to room temperature, the mixture was filtered, and the filtrate was distilled under vacuum to remove the methanol. The residue was extracted with dichloromethane (3 × 20 mL), dried over Na_2SO_4, and concentrated to give the product **5** (2.12 g, 91%) as white solid, which was stored under nitrogen condition. ^{1}H NMR (400 MHz, CD_3SOCD_3) δ 6.39 (s, 1H), 6.36 (s, 2H), 4.97 (s, 2H), 3.34 (s, 4H), 3.29-3.21 (m, 16H), 2.34-2.29 (m, 8H), 1.85-1.76 (m, 4H), 1.75-1.63 (m, 8H), 1.38 (s, 36H). ^{13}C NMR (101 MHz, $CDCl_3$) δ 155.41, 145.48, 139.55, 119.26, 113.46, 78.46, 57.84, 49.21, 44.15, 42.83, 27.64, 26.55, 25.84. IR (KBr, cm^{-1}): 3450, 2974, 2932, 2792, 1692, 1477, 1416, 1366, 1305, 1253, 1170, 1142, 1065, 868, 773. HR-MS (ES^+) Cacld. for $C_{46}H_{82}N_7O_8(M+H)^+$: 860.6225, found: 860.6229.

*4.3.3 Preparation of compound **1a***[48]

To a mixture of triethylamine (0.12 g, 1.16 mmol) and triphosgene (0.69 g, 0.23 mmo) in 10 mL of dichloromethane was added compound **5** (0.50 g, 0.58 mmol) under ice-bath condition. A solution of compound **6** (0.25 g, 0.58 mmol) in 2 mL of dichloromethane was added to the mixture. The reaction mixture was stirred for 10 h at room temperature. The solvent was removed by reduced pressure, and the residue was extracted with dichloromethane and dried over anhydrous Na_2SO_4. After removal of the solvent, the crude product was purified over silica gel using dichloromethane/methanol (10/1) as the eluent to give the inermediate as yellow solid (0.1 g), which was added to a saturated HCl/ethyl acetate solution (5 mL). After 0.5 h of stirring, the resulting suspension was filtered, washed with ethyl acetate, and dried in vacuum at 60 °C for 24 h to give compound **1a** (80 mg, 17%) as yellow solid. ^{1}H NMR (400 MHz, D_2O) δ 8.27 (s, 1H), 8.13 (s, 1H), 7.95 (s, 1H), 7.48 (s, 2H), 7.38 (s, 1H), 7.19 (s, 1H), 6.22 (s, 1H), 4.22 (s, 2H), 3.77 (s, 2H), 3.75-3.30 (m, 20H), 3.02 (s, 4H), 2.38-2.13 (m, 12H), 1.84-0.58 (m, 24H), 0.50 (s, 3H); ^{13}C NMR (101 MHz, D_2O) δ 164.61, 163.77, 156.69, 156.27, 150.52, 140.95, 139.81, 130.55, 130.25, 129.17, 128.31, 126.96, 123.53, 122.66, 121.22, 119.73, 107.52, 103.59, 58.26, 52.88, 46.76, 42.21, 42.10, 41.06, 40.96, 31.26, 29.47, 28.35, 27.10, 26.71, 22.26, 20.58, 20.47, 17.54, 17.39, 13.70; IR (KBr, cm^{-1}): 3425.58, 2927.94, 2852.72, 1676.14, 1633.71, 1573.91, 1467.83, 1388.75, 1246.02, 1112.93, 773.46; HR-MS (ES^+) calcd. For $C_{53}H_{84}N_{10}O_3$ $(M+H)^+$: 909.6728, found 909.6807.

*4.3.4 Preparation of compound **1b***[30]

Oleic acid (0.28 g, 1.00 mmol), EDCI (0.23 g, 1.20 mmol), BtOH (0.17 g, 1.20 mmol) and DIEA (0.25 g, 2.00 mmol) were added into dichloromethane (10 mL). After stirring for 0.5 h, compound **5** (0.86 g, 1.00 mmol) was added to the reaction mixture and stirred for 12 h. The mixture was extracted with dichloromethane (3 × 15 mL). The organic phase was dried (Na_2SO_4), filtered, and the solvent was evaporated under reduced pressure. The crude material was purified by column chromatography on silica gel (dichloromethane/methanol = 10/1) to give a white solid, which was reacted with a saturated HCl/ethyl acetate solution to give compound **1b** (0.53 g, 56%) as white solid. ^{1}H NMR (400 MHz, D_2O) δ 7.80 (s, 2H), 7.45 (s, 1H), 5.29 (s, 2H), 4.31 (s, 4H), 3.37 (s, 24H), 2.44-2.18 (m, 14H), 2.05-1.85 (m, 4H), 1.61 (s, 2H), 1.29-1.19 (m, 20H), 0.82 (t, *J* = 6.6 Hz, 3H); ^{13}C NMR (101 MHz, D_2O) δ 174.74, 139.60, 129.96, 129.67, 124.12, 57.69, 47.16, 42.33, 41.17, 36.89, 31.85, 29.69, 29.49, 29.29, 29.24, 29.15, 27.19, 27.10, 25.45, 22.60, 20.46, 17.93, 13.98; IR (KBr, cm^{-1}): 3425.58, 2926.01, 2852.72, 1606.43, 1562.34, 1463.97, 1361.03, 1209.37, 1070.49, 742.59, 547.76; HR-MS (ES^+) calcd. For $C_{44}H_{81}N_7O_3$ $(M+H)^+$: 724.6503, found 724.6577.

*4.3.5 Preparation of compound **1c***

Compound **1c** was synthesized according to a similar method with earlier report[30]. Briefly, compound **8** (0.23 g, 1.00 mmol) was reacted with octadecan-1-amine (0.27 g, 1.00 mmol) in the presence of EDCI (0.23 g, 1.20 mmol), BtOH (0.17 g, 1.20 mmol) and DIEA (0.25 g, 2.00 mmol). After reaction finished, the crude material was obtained by simple purification, which was directly reacted with compound **9** (0.82 g, 2.00 mmol) in THF-H_2O (10 mL/5 mL). The mixture was stirred overnight at room temperature. The solvent was removed under reduced pressure, and the residue was extracted with dichloromethane (3 × 20 mL). The Boc-protected compound was purified by column chromatography to give white solid, which was reacted with a saturated HCl/ethyl acetate solution to give compound **1c** (0.32 g, 27%) as yellow solid. ^{1}H NMR (400 MHz, D_2O) δ 8.23 (s, 2H), 7.75 (s, 2H), 7.27 (s, 1H), 5.53 (s, 4H),

4.11 (s, 4H), 3.32 (s, 18H), 3.00 (s, 8H), 2.24 (s, 4H), 2.07 (s, 8H), 1.50 (s, 2H), 1.19 (s, 30H), 0.80 (s, 3H); ^{13}C NMR (101 MHz, D_2O) δ 167.47, 138.61, 136.33, 135.47, 130.65, 127.30, 127.10, 53.28, 49.01, 47.00, 43.24, 42.02, 40.22, 31.94, 29.88, 29.43, 29.20, 27.14, 22.65, 20.09, 19.38, 14.01; IR (KBr, cm^{-1}): 3423.65, 2924.09, 1637.56, 1602.85, 1460.11, 1362.96, 1238.30, 1116.78, 1058.92, 744.52, 582.50; HR-MS (ES^+) calcd. For $C_{51}H_{91}N_{13}O$ $(M+H)^+$: 902.7470, found 902.7542.

4.4 Agarose gel retardation assays

Lipid/DOPE/pDNA complexes at different concentrations were prepared by adding appropriate volume of the liposome solution to 0.9 μL of pUC18 DNA (200 μg/mL) and 4 μL of HEPES (50 mM，pH 7.4). The obtained complex solution was then diluted to the total volume of 20 μL. After incubation at 37 °C for 5 min, 10 μL of each lipoplex solution was electrophoresed on a 0.7 % (w/v) agarose gel containing Gold view in Tris-acetate (TAE) running buffer at 120 V for 30 min. Then DNA was visualized under an ultraviolet lamp using a Vilber Lourmat imaging system.

4.5 Dynamic light scattering (DLS)

The liposome/DNA complexes were prepared by adding pUC18 DNA (4 μg/mL) to the appropriate volume of the liposome solution. The complex solution was then vortexed for 30 s before being incubated at 37 °C for 5 min and was measured at 25 °C. Data were shown as average of four times measurements.

4.6 Scanning electron microscope (SEM) images

0.9 μL of pUC18 DNA (200 μg/mL) was mixed with the appropriate volume of liposomes solution to form complexes, diluted by water to a total volume of 20 μL, and incubated at 37 °C for 5 min. The lipoplexes were added dropwise to the silicon slice. The slice was then dried at room temperature at atmospheric pressure for several hours before observation.

4.7 Cytotoxicity assays

The cytotoxicity of lipoplexes towards A549, HeLa, U2Os and SKOV-3 cell lines were tested by MTT assays[43]. The cells were seeded in 96-well plates at 7000 cells and 100 μL medium per well and cultured for 24h. The cells were then treated with different N/P ratios of liposomes **1a-1c** in 100 μL DMEM. After a 4h co-incubation, 100 μL DMEM with 10% FBS was added to each well and cells were further cultured for 24h. After that the medium was removed and 10 μL of MTT (5 mg/mL) was added to wells. Finally, MTT was replaced with 150 μL of DMSO. The optical density (OD) of the medium was measured by a microplate reader at 490 nm.

4.8 In vitro gene transfection

Luciferase assay[36]. The *in vitro* transfections mediated by the plasmid pGL-3-containing complexes were conducted A549, HeLa, U2Os, SKOV-3 and E1 cells. Briefly, cells were seeded in 24-well plates and cultured until reach 70-80% cell confluence. After a 4 h co-incubation and subsequent removal of the medium, the cells were further cultured in fresh DMEM medium containing 10% FBS for 20 h. The gene transfection efficiency of each sample was represented by firefly luciferase expression and calculated as relative light units per milligram of the total protein.

Green fluorescent protein assay[36]. To examine the expression of the internalized DNA, A549 cells were transfected by the condensates containing pEGFP-N1. Cells were seeded in glass bottom cell culture dishes and cultured until 80% cell confluence. Before transfection, the medium was washed three times with DMEM, and treated with freshly prepared pEGFP-DNA condensates and the controls (500 μL). After 4 h under standard culture conditions, the medium was replaced with 500 μL of fresh DMEM medium containing 10% FBS. After 20h incubation, the cells were washed for 3 times with PBS, and observed under Zeiss Inverted Fluorescence Microscope with a 10 × objective to examine the expression of the intracellular EGFP.

4.9 Cellular uptake assays

The cellular uptake of **1a**/Cy5-DNA condensates was observed with or without FBS by fluorescence microscope[30]. A549 cells were cultured in DMEM medium with 10% FBS in at 37 °C. The cells were seeded at a density of 10^3 cells per dish and cultured for 24 h. After washed three times with DMEM, the cells were treated with **1a**/Cy5-DNA condensates (**1a**: 30 μM, Cy5-DNA: 9 μg/mL). The blue fluorescence dye DAPI (5 μg/mL) was also added to each dish for nuclear staining, after that the cells were cultured for 2 h. Finally, the cells were washed for 6 times with PBS buffer, observed using a Zeiss Inverted Fluorescence Microscope with a 40 × objective and DAPI filter for DAPI (blue), GFP filter for lipid **1a** (green), and Rhodamine filter for Cy5 (red), respectively.

4.10 Mechanism Studies

To probe the internalization mechanism of the lipoplexe **1a**, the cellular uptake study was performed at 4 °C or in the presence of various endocytic inhibitors[44, 45]. Briefly, cells were incubated with **1a**/pUC18 DNA complexes (10 μM) at 4 °C for 4 h, the energy-dependent endocytosis was completely blocked. Otherwise, cells were preincubated with various endocytic inhibitors including chlorpromazine (20 μg/mL), cytochalasin D (10 μg/mL), genistein (200 μM), and nocodazole (33 μM). Following pretreatment for 2h, the inhibitor solutions were replaced by the **1a**/pUC18 DNA complexes (10 μM). After further incubation for 2 h, the cells were washed 6 times with PBS buffer and were observed using a Zeiss Inverted Fluorescence Microscope with a 10 × objective.

Acknowledgments

The authors gratefully acknowledge the financial assistance provided by the National Natural Science Foundation of China (31570940, 31400725, 81700784 and 21372032).

References

1. Keeler, A. M.; Elmallah, M. K.; Flotte, T. R. *Clin. Transl. Sci.* 2017, *10*, 242-248.
2. Viswam, S.; Chithra, J.; Surendran, S. A. *Int. J. Pharm. Sci. Rev. Res.* 2015, *31*, 14-17.
3. Azvolinsky, A. *Nat. Biotechnol.* 2015, *33*, 678-678.
4. McMahon, M. A.; Cleveland, D. W. *Nat. Rev. Neurol.* 2017, *13*, 7-9.
5. Anderson, W. F. *Nature* 1998, *392*, 25-30.
6. Miller, H. L. *Science* 2015, *348*, 1325.
7. Mulligan, R. C. *Science* 1993, *260*, 926-932.
8. O'Connor, D. M.; Boulis, N. M. *Trends Mol. Med.* 2015, *21*, 504-512.
9. Verma, I. M.; Somia, N. *Nature* 1997, *389*, 239-242.
10. Luo, J.; Luo, Y.; Sun, J.; Zhou, Y.; Zhang, Y.; Yang, X. *Cancer Lett.* 2015, *356*, 347-356.
11. Schoen, C.; Biel, M.; Michalakis, S. *Eur. J. Pharm. Biopharm.* 2015, *95*, 343-352.
12. Kay, M. A.; Glorioso, J. C.; Naldini, L. *Nat. Med.* 2001, *7*, 33-40.
13. Waehler, R.; Russell, S. J.; Curiel, D. T. *Nat. Rev. Genet.* 2007, *8*, 573-587.
14. Pepin, D.; Sosulski, A.; Zhang, L.; Wang, D.; Vathipadiekal, V.; Hendren, K.; Coletti, C. M.; Yu, A.; Castro, C. M.; Birrer, M. J.; Gao, G.; Donahoe, P. K. *Proc. Natl. Acad. Sci. USA.* 2015, *112*, 4418-4427.
15. Thomas, C. E.; Ehrhardt, A.; Kay, M. A. *Nat. Rev. Genet.* 2003, *4*, 346-358.
16. Guo, X.; Huang, L. *Acc. Chem. Res.* 2012, *45*, 971-979.
17. Jia, H. Z.; Zhang, W.; Wang, X. L.; Yang, B.; Chen, W. H.; Chen, S.; Chen, G.; Zhao, Y. F.; Zhuo, R. X.; Feng, J.; Zhang, X. Z. *Biomater. Sci.* 2015, *3*, 1066-1077.
18. Mintzer, M. A.; Simanek, E. E. *Chem. Rev.* 2009, *109*, 259-302.
19. Yang, J.; Zhang, Q.; Chang, H.; Cheng, Y. *Chem. Rev.* 2015, *115*, 5274-5300.
20. Hardee, C. L.; Arévalosoliz, L. M.; Hornstein, B. D.; Zechiedrich, L. *Genes* 2017, *8*, 65.
21. Xu, H.; Li, Z.; Si, J. *J. Biomed. Nanotechnol.* 2014, *10*, 3483-3507.
22. Ramamoorth, M.; Narvekar, A. *J. Clin. Diagn. Res.* 2015, *9*, GE01-GE06.
23. Gashti, A. B.; Prakash, H. S. *J. Pharm. Res.* 2012, *5*, 4361-4365.
24. Yin, H.; Kanasty, R. L.; Eltoukhy, A. A.; Vegas, A. J.; Dorkin, J. R.; Anderson, D. G. *Nat. Rev. Genet.* 2014, *15*, 541-555.
25. Liu, B.; Liu, Q.; Zhang, J.; Fan, S.; Yu, X. *Prog. Chem.* 2013, *25*, 1237-1245.
26. Singh, J.; Mohammed-Saied, W.; Kaur, R.; Badea, I. *Rev. Nanosci. Nanotechnol.* 2013, *2*, 275-299.
27. Chang, D. C.; Zhang, Y. M.; Zhang, J.; Liu, Y. H.; Yu, X. Q. *Rsc Advances* 2017, *7*, 18681-18689.
28. Felgner, P. L.; Holm, M.; Chan, H. *Nature* 1989, *337*, 387-388.
29. Zhi, D.; Zhang, S.; Wang, B.; Zhao, Y.; Yang, B.; Yu, S. *Bioconjugate Chem.* 2010, *21*, 563-577.
30. Gao, Y. G.; Shi, Y. D.; Zhang, Y.; Hu, J.; Lu, Z. L.; He, L. *Chem. Commun.* 2015, *51*, 16695-16698.
31. Ding, A.; Tang, Q.; Gao, Y. G.; Shi, Y. D.; Uzair, A.; Lu, Z. L. *Acs Appl. Mater. Interfaces* 2016, *8*, 14367-14378.
32. Gao, Y. G.; Uzair, A.; Tang, Q.; Shi, Y. D.; Zhang, Y.; Wang, R.; Lu, Z. L. *Org. Biomol. Chem.* 2016, *14*, 6346-6354.
33. Yue, P.; Zhang, Y.; Guo, Z. F.; Cao, A. C.; Lu, Z. L.; Zhai, Y. G. *Org. Biomol. Chem.* 2015, *13*, 4494-4505.
34. Radaram, B.; Levine, M. *Tetrahedron Lett.* 2014, *55*, 4905-4908.
35. Guo, Z. F.; Yan, H.; Li, Z. F.; Lu, Z. L. *Org. Biomol. Chem.* 2011, *9*, 6788-6796.
36. Huang, Z.; Liu, Y. H.; Zhang, Y. M.; Zhang, J.; Liu, Q.; Yu, X. Q. *Org. Biomol. Chem.* 2015, *13*, 620-630.
37. Draghici, B.; Ilies, M. A. *J. Med. Chem.* 2015, *58*, 4091-4130.
38. Shoji-Moskowitz, Y.; Asai, D.; Kodama, K.; Katayama, Y.; Nakashima, H. *Front. Med. Chem.* 2010, *5*, 81-97.
39. Vijayanathan, V.; Thomas, T.; Thomas, T. J. *Biochem.* 2002, *41*, 14085-14094.

40. Yi, W. J.; Zhang, Q. F.; Zhang, J.; Liu, Q.; Ren, L.; Chen, Q. M.; Guo, L.; Yu, X. Q. *Acta Biomater*. 2014, *10*, 1412-1422.
41. Hemp, S. T.; Smith, A. E.; Bryson, J. M.; Jr, M. H. A.; Long, T. E. *Biomacromolecules* 2012, *13*, 2439-2445.
42. Yi, W. J.; Yu, X. C.; Wang, B.; Zhang, J.; Yu, Q. Y.; Zhou, X. D.; Yu, X. Q. *Chem. Commun.* 2014, *50*, 6454-6457.
43. Wang, B.; Zhao, R. M.; Zhang, J.; Liu, Y. H.; Huang, Z.; Yu, Q. Y.; Yu, X. Q. *Eur. J. Med. Chem.* 2017, *136*, 585-595.
44. Jin, Y.; Wang, S.; Tong, L.; Du, L. *Colloid. Surface. B* 2015, *126*, 257-264.
45. Kam, N. W. S.; Liu, Z.; Dai, H. *Angew. Chem. Int. Ed.* 2006, *45*, 577-581.
46. Zhang, Q.-F.; Yu, Q.-Y.; Geng, Y.; Zhang, J.; Wu, W.-X.; Wang, G.; Gu, Z.; Yu, X.-Q. *ACS Appl. Mater. Inter.* 2014, *6*, 15733-15742.
47. Kuchelmeister, H. Y.; Schmuck, C. *Eur. J. Org. Chem.* 2010, *2009*, 4480-4485.
48 Lee, M. H.; Kim, J. Y.; Han, J. H.; Bhuniya, S.; Sessler, J. L.; Kang, C.; Kim, J. S. *J. Am. Chem. Soc.* 2012, *134*, 12668− 12674.

Fig. 1. Agarose gel electrophoresis of liposomes **1a-1c** complexed with DNA to form lipoplexes at different concentrations; Condition: pUC18 DNA (9 μg/mL), HEPES (50 mM, pH 7.4), 37 °C, 5 minutes.

Fig. 2. The effective diameter of liposomes of **1a-1c**/DNA complexes at different concentrations, [DNA] = 9 μg/mL, HEPES buffer (50 mM, pH 7.4), 25 °C.

Fig. 3. SEM Images of pUC18 DNA (9 μg/mL) and its condensation induced complexes of **1a** with DOPE (1:2) at different concentrations in HEPES buffer (50 mM, pH 7.4).

Fig. 4. Cytotoxicity of liposomes **1a** (A), **1b** (B) and **1c** (C) at different concentrations toward A549, HeLa, U2Os and SKOV-3 cell lines, with lipofectamine 2000 (10 μg/mL) as the control.

Fig. 5. Luciferase gene expression transfected by (A) **1a**, **1b** and **1c** at different concentrations toward A549 cells, (B) **1a**, **1b** and **1c** at a concentration of 30 μM toward different cell lines, (C) **1a** at a concentration of 30 μM in the absence or presence of serum toward A549 cells.

Fig. 6. Fluorescence microscope image of pEGFP-transfected A549 cells of liposomes **1b** (30 μM), **1c** (30 μM) and Lipo2000 (10 μg/mL)

Fig. 7. CLSM images of A549 cells transfected with Cy5-labaled DNA (9 μg/mL) by **1a**/DOPE (1:2) at 30 μM in the absence (A) and presence of 10%, 30% and 50% serum. A: BF; B: cell stained by **1a** (green); C: Cy5-labeled DNA (red); D: cell nuclei stained by DAPI (blue); E: merged images.

Fig. 8. CLSM images of A549 cells at 37 °C, 4 °C and in the presence of various endocytic inhibitors. 1: BF; 2: cell stained by **1a** (10 μM); 3: merged images.

Scheme 1. The synthesis of cationic lipids **1a**, **1b** and **1c**